

Fabrication of Collagen Gel Hollow Fibers by Covalent Cross-Linking for Construction of Bioengineering Renal Tubules

Chong Shen,[†] Guoliang Zhang,[‡] Qichen Wang,[§] and Qin Meng^{*,†}

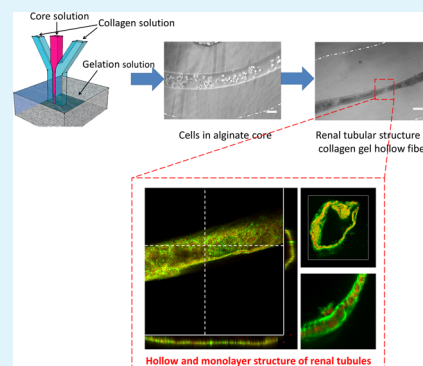
[†]Department of Chemical and Biological Engineering, Zhejiang University, Hangzhou 310027, China

[‡]College of Chemical Engineering and Materials Science, Zhejiang University of Technology, Hangzhou 310023, China

[§]Department of Chemical Engineering and Materials Science, Stevens Institute of Technology, Hoboken, New Jersey 07030, United States

ABSTRACT: Collagen, the most used natural biomacromolecule, has been extensively utilized to make scaffolds for cell cultures in tissue engineering, but has never been fabricated into the configuration of a hollow fiber (HF) for cell culture due to its poor mechanical properties. In this study, renal tubular cell-laden collagen hollow fiber (Col HF) was fabricated by dissolving sacrificial Ca-alginate cores from collagen shells strengthened by carbodiimide cross-linking. The inner/outer diameters of the Col HF were precisely controlled by the flow rates of core alginate/shell collagen solution in the microfluidic device. As found, the renal tubular cells self-assembled into renal tubules with diameters of 50–200 μm post to the culture in Col HF for 10 days. According to the 3D reconstructed confocal images or HE staining, the renal cells appeared as a tight tubular monolayer on the Col HF inner surface, sustaining more 3D cell morphology than the cell layer on the 2D flat collagen gel surface. Moreover, compared with the cultures in either a Transwell or polymer HF membrane, the renal tubules in Col HF exhibited at least 1-fold higher activity on brush border enzymes of alkaline phosphatase and γ -glutamyltransferase, consistent with their gene expressions. The enhancement occurred similarly on multidrug resistance protein 2 and glucose uptake. Such bioengineered renal tubules in Col HF will present great potential as alternatives to synthetic HF in both clinical use and pharmaceutical investigation.

KEYWORDS: renal tubule, collagen gel hollow fiber, 3D culture, renal functions, bioartificial kidney



INTRODUCTION

As one of the most complex organs in humans, the kidney serves many physiological functions, including the excretion of wastes, reabsorption of vital nutrients, osmolality regulation, and hormone secretion inside the renal tubules. Renal failure, caused by acute kidney injury or chronic diseases such as diabetes mellitus, is usually fatal and irreversible.¹ At the same time, renal transplantation, the most acceptable therapy for renal failure so far, is extremely limited because of the scarcity of donor sources. Hemodialysis is the solely available alternative to partially replace the renal function of filtration in the clinic. However, the semipermeable polymer hollow fiber (HF) membranes that are used in hemodialysis devices to simulate the geometric tubular configuration cannot perform most renal functions in the absence of living cells.² This causes a high mortality rate of >20% per year in the hemodialysis-treated patients, and average costs over \$70,000 annually for each patient.³

Aiming to improve renal function, renal cells have been loaded into hemodialysis devices, whereas renal tubular cells were cultured on the inner surface of polymer HF membranes to form a tubular cell monolayer.⁴ Nevertheless, this device still expressed low renal function due to the poor biocompatibility of synthetic HF membranes, which caused failure in its clinical application.⁵ In this respect, much research effort has been

made to improve the biocompatibility of HF membranes. For example, the membranes have been coated with extracellular matrix (e.g., collagen) or adhesive molecules (e.g., 3,4-dihydroxy-L-phenylalanine), providing cell recognizing/adhesive sites.⁶ Further, new membrane materials have also been prepared via blending adhesive molecules (e.g., acrylic-based polymer)⁷ or hemocompatible molecules (e.g., phosphorylcholine containing polymer)⁸ into the polymers. However, these efforts have not obtained substantial improvement due to the fact that the synthetic polymers dominate the membrane composites.

Inside the kidney, the renal tubules are surrounded and supported by the extracellular matrix of natural macromolecules. The most abundant extracellular matrix in a kidney is collagen, a soft and hydrated biomacromolecule, which comprises triple-helix amino acid fiber structures. Collagen, unlike the synthetic membranes, possesses plenty of cell recognizing sites so that it plays an important role in forming cell basement membranes,⁹ regulating cell mechanotransduction,¹⁰ and repairing physiological functions after toxicant injury.¹¹ Therefore, collagen has been well-known for the

Received: June 30, 2015

Accepted: August 17, 2015

Published: August 17, 2015

highest cell compatibility and is extensively used in constructing bioartificial organs for kidney, liver, and skin.¹²

Homogenous collagen gel has been used for immobilizing renal tubular cells, but it only promotes the cells to form cysts or random short branches instead of regular tubules.¹³ Therefore, a collagen gel at a configuration of hollow fiber (Col HF) might be able to successfully promote the formation of renal tubules like synthetic HF membranes do. However, the thermogelling collagen is too soft to be directly fabricated into HF, like some other hydrogel materials (e.g., alginate).¹⁴ The covalent cross-linking by chemicals such as 1-ethyl-3-(3-(dimethylamino)propyl) carbodiimide hydrochloride (EDC) can improve the mechanical property of collagen,¹⁵ but such a strategy has rarely been used in the fabrication of either particular shape (e.g., HF) or cell-laden collagen.

In this paper, a cell-laden Col HF is generated in a microfluidic device under coaxial flow, and its mechanical stability is further enhanced by EDC cross-linking. The bioengineered renal tubules with high physiological function are formed after the cell self-assembly into the lumen of Col HF. The differentiation of renal cells is assessed by assay of brush border enzyme activities,¹⁶ and their reabsorption abilities are represented by multidrug resistance protein 2 (MRP2) activity and glucose uptake.¹⁷ Such cell-laden Col HF in mimicking the renal tubules in vivo from both material components and spatial structures can be potentially developed into an alternative to synthetic HF in tissue engineering applications.

MATERIALS AND METHODS

Materials. Sodium alginate powder, fluorescein diacetate (FDA), propidium iodide (PI), 5-carboxyfluorescein diacetate (5-CFDA, AM), Alexa Fluor488 phalloidin, and DMEM/F12 medium were purchased from Sigma-Aldrich Chemical Co. (St. Louis, MO, U.S.A.). L-Glutamine, bovine serum albumin (BSA, Fraction V), and methyl thiazolyltetrazolium (MTT) were purchased from Amresco Inc. (Solon, Ohio, U.S.A.). Fetal bovine serum (FBS) was obtained from Gibco (Invitrogen Co. Ltd., Canada). Collagen sponge (type I, from bovine achilles tendon) was purchased from Biot Biology Inc. (Wuxi, China). 1-Ethyl-3-(3-(dimethylamino)propyl) carbodiimide hydrochloride (EDC) and *N*-hydroxysuccinimide (NHS) were purchased from Aladdin Reagent Inc. (Shanghai, China). The *L*- γ -glutamine-4-nitroanilide and glucose colorimetric assay kit were purchased from Saik Bio. Inc. (Ningbo, China). RNA isolation kit, first strand cDNA synthesis kit and other PCR reagents were purchased from Takara Bio. Inc. (Otsu, Japan). Primers were synthesized by Sangong Co., Ltd. (Shanghai, China). The remaining chemicals were obtained from local chemical suppliers and were all of reagent grade.

Fabrication of Col HF. As shown in Figure 1, a polydimethylsiloxane (PDMS) microfluidic device with 2 inlet channels (330 μm in width) and a straight outlet channel (500 μm in width) was first fabricated via standard soft lithography and replica molding techniques.¹⁸ To make the cell-free or cell-laden Col HF, the same microfluidic device was used with different core, shell, and gelation solution as listed in Table 1. The core and shell solution was continuously injected into the corresponding inlets, mixed in microfluidic channels, and then flowed out from an outlet which was immersed in gelation solution. After fabrication, the formed collagen fibers were kept in gelation solution for 3 h for complete cross-linking. For the Ca-alginate core fibers, the fibers were further soaked in 55 mM sodium citrate solution for 30 min to liquefy the Ca-alginate. The cell-laden Col HF was cultured into DMEM/F12 medium containing 10% FBS and placed into an incubator.

Characterization of Cell-Free Col HF. The tensile strength represented by Young's modulus of Col HF cross-linked by different EDC concentrations was detected on an Instron Series IX Automated

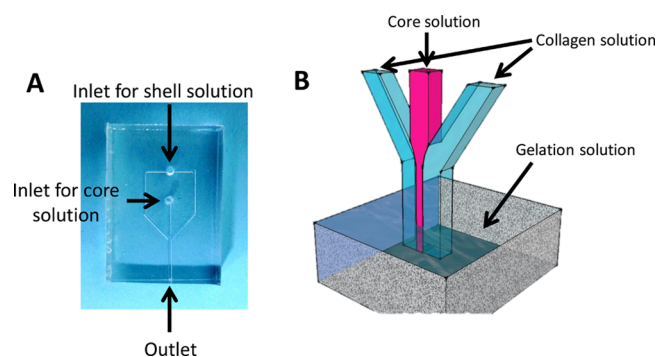


Figure 1. Image (A) and explanatory illustration (B) of the microfluidic device for fabrication of collagen gel hollow fibers.

Materials Testing System following the previously reported method.^{15a} A crosshead speed of 5 mm/min and full-scale load range of 500 N were used for the test at room temperature and humidity of 50%.

The Col HF cross-linked by 20 mM EDC was fully rinsed by deionized water and dried in atmosphere at room temperature on a glass slide. The dried samples were carefully torn down and analyzed by Fourier transform infrared/attenuated total reflection (FTIR/ATR) spectra. The un-cross-linked collagen solution was poured onto a glass slide and similarly dried and analyzed as a control.

Cell Culture on 2D Flat Collagen Gel Surface, Transwell Insert, and HF Membranes. The HK-2 cell culture on a 2D flat collagen gel surface was set to compare the cell morphology in Col HF. For this culture, collagen solution (2% w/v) was first cross-linked by 20 mM of EDC and NHS, and then the HK-2 cells were seeded onto the surface of the gel at a density of 2×10^5 cells/cm².

The cultures of Transwell insert and HF membranes were used as control groups for cell functional assay. For the Transwell culture, the cells were seeded on the Transwell insert (Cat. No. 3415, Corning Inc., New York) at a density of 2×10^5 cells/cm². For the cell culture on synthetic HF membranes, the HK-2 cells at a density of 1×10^7 cells/mL were loaded into the lumen of HF membranes with inner diameters of 0.4 mm, as described in our previous study.¹⁹ For each culture, the medium was changed every 2 days.

Assay on Cell Viability and Proliferation. The FDA/PI staining was used for direct observation of living/dead cells. After 3 h of incubation with FDA/PI solution (10 μM for each fluorescent probe in PBS), the HK-2 cells in fibers were washed three times in PBS and imaged under a fluorescence microscope (OLYMPUS Ix70) with green/red fluorescent excitors and a bright field light source at the same time.

The MTT reduction was used to evaluate the viability of HK-2 cells. Briefly, the cells were rinsed by PBS before being immersed in 1 mL of the MTT-phosphate buffer solution (PBS) at 1.15 mg/mL. After being incubated at 37 $^{\circ}\text{C}$ for 3 h, the cells were washed by PBS and then added to 1.5 mL of acidified isopropanol. After agitation for 1 h, the extraction was measured at an absorbance of 570 nm on a spectrophotometer.

The cell proliferation in Col HF was represented by the increased total proteins in cell-laden Col HF. After the cell-laden Col HF was lysed by 1% Triton X-100, the protein concentrations in the lysis solution were measured by BCA protein assay kit. The amount of cells were displayed as the amount of total proteins (mg) in 1 g Col HF.

Cell Morphology Observation. After 10 days of culture, HK-2 cells in Col HF were observed by cytoskeleton staining, hematoxylin–eosin (HE), and immunofluorescence staining.

The Col HF with cells inside was fixed by 4% paraformaldehyde and cut into 5-mm long segments. The cytoskeleton was stained with Alexa Fluor488 phalloidin, and the nucleolus was stained with propidium iodide (PI) following the manufacturer's protocol. The stained cells were imaged by confocal microscopy (Nikon E-1000 + C1 LSCM) in two- and three-dimensions.

For HE staining, the cell specimens were embedded into paraffin and sectioned into 8 μm thick slices before subsequent staining with

Table 1. Parameters for Fabrication of Collagen Gel Hollow Fiber (Col HF)

| description of Col HF | core solution | shell solution | gelation solution | renal cells | purpose of experiment design |
|---------------------------------|--|---|---|--|--|
| cell-free | culture medium, 50 $\mu\text{L}/\text{min}$ | 2 w/v% collagen in PBS, 50–350 $\mu\text{L}/\text{min}$ | HBSS with EDC and NHS (both 20 mM) | no cells | determine the relationship between Col HF diameters and flow rates |
| cell-laden, without Ca-alginate | culture medium, 50 $\mu\text{L}/\text{min}$ | 2 w/v% collagen in PBS, 50 $\mu\text{L}/\text{min}$ | HBSS with EDC and NHS (0.4–50mM, molar ratio of 1:1) | 5×10^6 cells/mL, in core solution | test cross-linking effect and cytotoxicity of EDC |
| cell-laden, Ca-alginate core | 2 w/v% Na-alginate in PBS, 50 $\mu\text{L}/\text{min}$ | 2 w/v% collagen in PBS, 50 $\mu\text{L}/\text{min}$ | HBSS with CaCl_2 , 11.1 g/L, EDC and NHS (0.4–50 mM, molar ratio of 1:1) | 5×10^6 cells/mL, in core solution | avoid EDC cytotoxicity by Ca-alginate protection |

HE. The slices were observed using a common inverted phase contrast microscope.

For immunofluorescence staining, the sectioned paraffin sample slices were dewaxed and blocked in 10% fish skin gelatin in PBS. Samples were incubated overnight at 4 °C with collagen IV primary antibodies. After three rinses with PBS, incubation with Alexa Fluor 594 goat-antirabbit secondary antibody (Invitrogen) was performed for 1 h at room temperature. Nuclear staining was performed by mounting medium containing DAPI (Vector Laboratories). Confocal microscopy (Carl Zeiss LSM 5 Exciter) was used to visualize stained cells.

Measurement of Brush Border Enzyme Activities. Alkaline phosphatase (ALP) and γ -glutamyltransferase (GGT) were assessed to represent the activity of brush border enzymes in HK-2 cells. ALP activity was measured as previously reported.²⁰ Briefly, HK-2 cells in each culture were respectively lysed using 1% Triton X-100, and then 20 μL of lysis solution was added to 100 μL reaction solution containing 0.5 M Tris, 10 mM *p*-nitrophenyl phosphate disodium, 2 mM MgCl_2 , and 1 mM ZnCl_2 at pH 10. After incubation at 37 °C for 30 min, the solution was added to 80 μL of NaOH (1 M) to terminate the reaction. The absorbance of the solution was read by a microplate reader at 405 nm. Similarly, GGT activity was assayed using an L- γ -glutamine-4-nitroanilide colorimetric kit.²¹

Determination of MRP2 Activity and Glucose Uptake. The activity of multidrug resistance protein 2 (MRP2) was represented by the efflux of 5-carboxyfluorescein diacetate (5-CFDA) in the presence or absence of probenecid.²² Briefly, HK-2 cells in each culture after 10 days of incubation were initially loaded with 10 μM 5-CFDA for 30 min and washed twice in ice-cold (0 °C) HBSS to terminate dye loading. Subsequently, cells were incubated in 500 μL of dye-free HBSS for 30 min at 37 °C in the presence or absence of 1 mM probenecid. The efflux of 5-CFDA from cells into HBSS was measured by fluorescence spectroscopy at 485/585 nm. MRP2 activity was represented by the differential efflux of 5-CFDA in the presence or absence of probenecid.

The glucose uptake by HK-2 cells was represented by the decreased glucose concentrations in medium in the presence or absence of the glucose transporter inhibitors.²³ After being rinsed three times using glucose-free PBS, HK-2 cells in each culture were incubated by HBSS-BSA solution (2.5 g/L of BSA) with or without 2 mM phlorizin, or incubated with Na^+ -free HBSS-BSA solution (2.5 g/L of BSA, replacing the NaCl with *N*-methyl-D-glucamine). After 120 min of incubation at 37 °C, the solution in each culture was sampled and analyzed for glucose concentrations using the glucose colorimetric assay kit. The glucose uptake was represented by the amount of glucose transported by mg protein per hour.

Gene Expression of Enzymes and Transporters in Cells. Total RNA was isolated from HK-2 cells after 10 days of incubation in each culture using a MiniBEST Universal RNA Extraction Kit. The quality of RNA was assessed by sample absorbance at 230, 260, and 280 nm. cDNA was synthesized as previously described²⁴ and amplified by the polymerase chain reaction (PCR), while tubes containing no template were used as negative controls. Gene expression was measured for alkaline phosphatase (ALP), gamma-glutamyltransferase 1 (GGT1), multidrug resistance protein 2 (MRP2), and glucose transporter 1 (GLUT1), while expression of glyceraldehyde-3-phosphate dehydrogenase (GAPDH) was used as a control. The sequence of the primers is listed in Table 2.

Statistical Analysis. All data from cell experiments were analyzed by means \pm SD from three independent experiments. Comparisons between multiple groups were performed with the ANOVA test by SPSS, or results from two different groups were tested with the unpaired Student *t* test. *P*-values less than 0.05 were considered statistically significant.

RESULTS

Fabrication of Mechanically Stable Cell-Free Col HF.

As shown in Figure 1, a simple microfluidic device was used to prepare cell-free Col HF. The inner diameters of Col HF were

Table 2. Primer Sequences Used for RT-PCR Analysis

| primer name | NCBI reference sequence | forward sequence (5'–3') | reverse sequence (5'–3') | product size (bp) |
|--------------|-------------------------|--------------------------|--------------------------|-------------------|
| <i>GAPDH</i> | NM_002046.4 | TCACCAGGGCTGCTTTTAAC | TGTGGTCATGAGTCCTTCCA | 479 |
| <i>ALP</i> | NM_000478.4 | TCAGAAGCTCAACACCAACG | GCTGGTAGGCGATGTCCTTA | 494 |
| <i>GGT1</i> | NM_001032364.2 | AAGGGTACAACCTTCTCCCGG | ATTGAACAGGATCCCGCTGA | 374 |
| <i>MRP2</i> | NM_000392.4 | AAAAGGCCTTCACCTCCATT | CAAGTCTGGGAGGAGAGCAC | 500 |
| <i>GLUT1</i> | NM_006516.2 | AGGAGGTTGGATGGGAGTG | AATGAACACAGGGCAGCTTG | 487 |

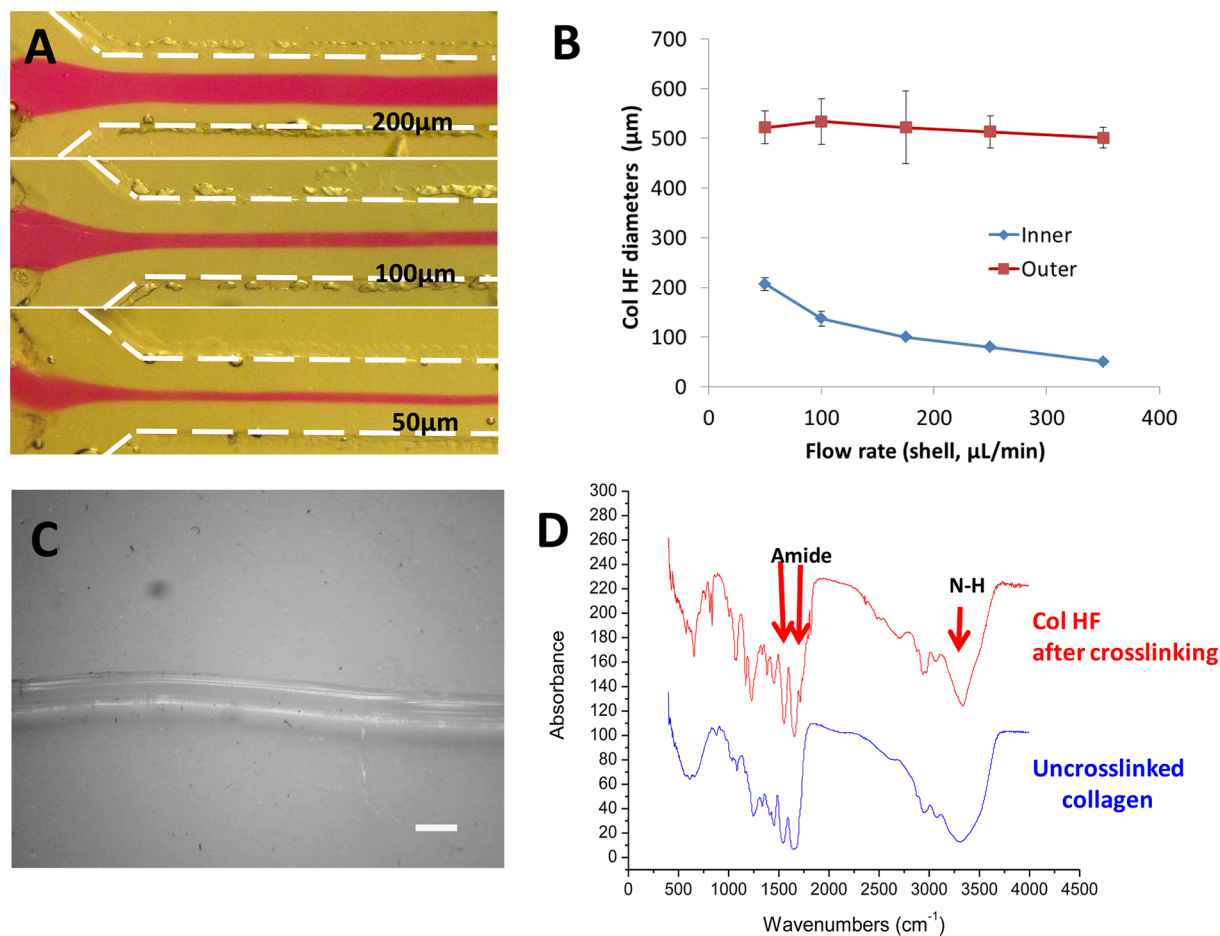


Figure 2. (A) Different core/shell laminar flow inside the microfluidic channel; (B) relationship between fiber inner/outer diameters of Col HF and shell flow rate; and (C) Col HF taken by camera. Scale bar = 500 μm ; (D) FTIR/ATR spectra of Col HF and un-cross-linked collagen. Col HF = collagen hollow fiber.

controlled by regulating the flow rate of the culture medium in the core side and the flow rate of the collagen solution in the shell side. As shown in Figure 2A, the core stream (stained by phenol red) had different diameters in the microfluidic channels under the regulation of core/shell flow rates. When the shell flow rate increased from 50 to 350 $\mu\text{L}/\text{min}$, the inner diameters of Col HF correspondingly decreased from 200 to 50 μm , while the outer diameters remained to be about 500 μm (Figure 2B).

Under sufficient EDC cross-linking, the obtained cell-free Col HF possessed a well-defined shape and can be observed by the naked eye (Figure 2C), suggestive of a stable mechanical property. This Col HF was further detected on FTIR/ATR spectra. As shown in Figure 2D, the Col HF had the higher intensity of amide absorbance bands (1550 and 1660 cm^{-1}) and the lower intensity of N—H stretching bands (3300–3400 cm^{-1}), in comparison to the un-cross-linked collagen, indicating the newly formed amide groups in the Col HF.

Evaluation of EDC Toxicity on Cell-Laden Col HF and Avoiding the Toxicity via Design of Ca-Alginate Core Fiber. Following the fabrication parameters of cell-laden Col HF in Table 1, the cross-linking by EDC at above 1 mM was severely toxic to cells in the Col HF lumen, while the cross-linking by EDC at 0.4 mM, although causing low cell toxicity, failed to sustain an appropriate Young's modulus (Figure 3A).

To avoid the EDC toxicity and to obtain mechanically stable Col HF as well, the Na-alginate was used as the core solution that could entrap cells after being cross-linked by Ca^{2+} to avoid direct contact with the EDC. As shown in Figure 3B, the entrapped HK-2 cells in the Ca-alginate core did survive after 3 h of EDC cross-linking up to 50 mM, with the toxic dose being enhanced over 100 fold. Under these fabrication conditions, the Young's modulus of Col HF (Figure 3B) was even higher than that with the culture medium core solution, being 0.24 over 0.2 MPa (Figure 3, parts A and B). The reduced EDC toxicity was also shown by FDA/PI staining in Figure 3C, where cells in the

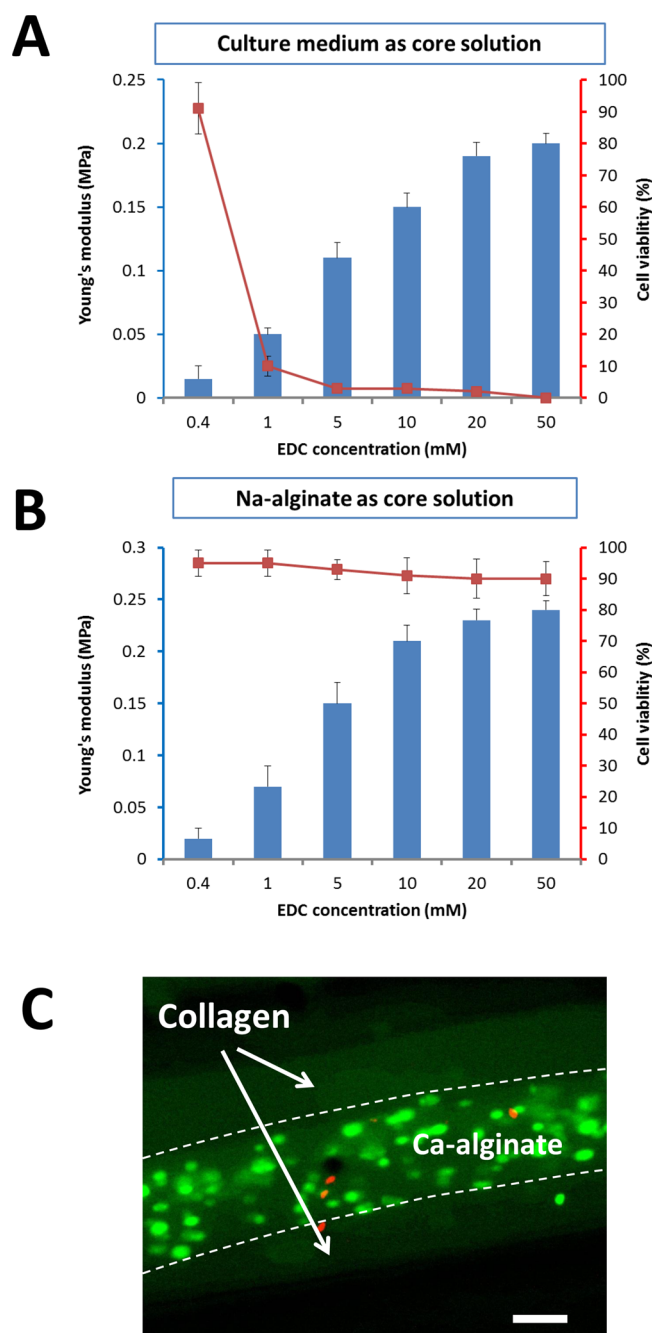


Figure 3. EDC dose dependent effects on cell viability and Young's modulus of Col HF with core solution of culture medium (A) and Na-alginate (B). Fluorescein diacetate/propidium iodide (FDA/PI) staining of HK-2 cells in Ca-alginate/collagen core-shell fibers after 3 h of cross-linking with 20 mM EDC (C). Living cells were stained green by FDA, whereas dead cells were stained red by PI. Scale bar = 100 μm. Col HF = collagen hollow fiber, EDC = 1-ethyl-3-(3-(dimethylamino)propyl) carbodiimide hydrochloride.

Ca-alginate core were mostly alive (stained green by FDA) with little cell death (stained red by PI). For further experiments, 20 mM of EDC was chosen as the optimized concentration because the higher dose of 50 mM did not significantly improve the Young's modulus of Col HF.

Self-Assembly of HK-2 Cells to Renal Tubules in Col HF. The morphology of HK-2 cells in the gelled core/shell hydrogel fibers is shown in Figure 4. Initially, the cells dispersed

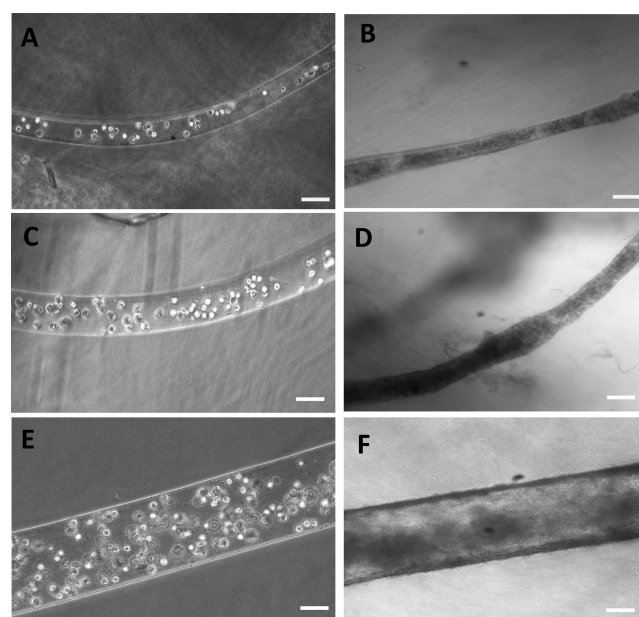


Figure 4. Morphology of HK-2 cells in Col HF with Ca-alginate core at diameters of 50 μm (A), 100 μm (C), and 200 μm (E), and after 10 days of culture in Col HF with inner diameters of 50 μm (B), 100 μm (D), and 200 μm (F). Scale bar = 50 μm. Col HF = collagen gel hollow fiber.

in the Ca-alginate core fibers with diameters of 50, 100, or 200 μm (Figure 4, parts A, C, and E). After being released to the inner surface of Col HF by exposure to Ca^{2+} chelating agent, the cells adhered onto the inner surface of Col HF and began to form a cell layer. At 10 days, the cells finally formed the intact tubules with different diameters along their corresponding lumen surfaces (Figure 4, parts B, D, and F), while the tubules in the Col HF lumen of 200 μm showed better uniformity in tubular diameters than those in the Col HF lumen of 50 and 100 μm.

The bioengineered renal tubules were further observed by confocal fluorescence micrography, where the F-actin was green and the nuclei were red (Figure 5). Figure 5A shows the cell self-assembly inside the Col HF. The cross section views of right and bottom images, which were optically sliced at the white dash lines, revealed that the tubular structure and cells only grew into monolayer on the fiber inner surface. The 3D reconstructed image (Figure 5B) clearly showed the ring-shape tubular structure of HK-2 cells in Col HF. The zoom-in image (Figure 5C) displayed the rearrangement of F-actin on the peripheral area of cell monolayer. These images and optical slides indicated that the HK-2 cells only attached, proliferated, and formed monolayer on the Col HF inner surface without invading into collagen or filling the lumen.

To examine the cell configuration in Col HF, the formed renal tubules were embedded in paraffin and sectioned to slices for HE and immunofluorescence staining while the HK-2 cell culture on flat collagen gel surface was set as a control (Figure 6). Consistent with the confocal images, a well-organized lumen of cell monolayer was observed in the cross-section of renal tubule (Figure 6A). The zoom in image in Figure 6B showed that the renal tubule was composed of tightly arrayed cells with thicknesses of about 10 μm. By contrast, the cells on the flat collagen gel performed as a monolayer line in the cross-section (Figure 6C), which was much thinner and had fewer nuclei than that in Col HF (Figure 6D), indicating that the cells

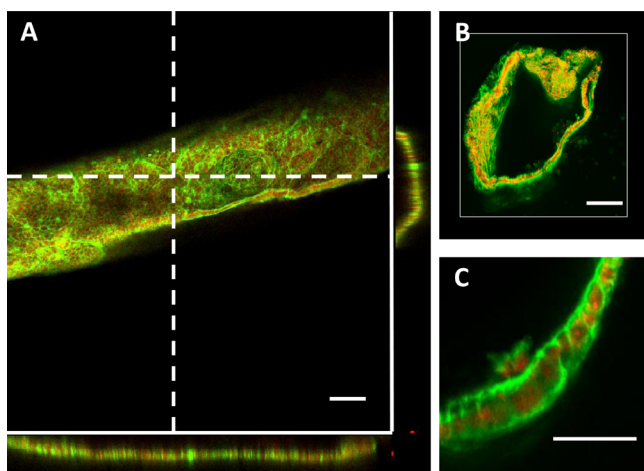


Figure 5. Confocal images of Alexa Fluor488-phallotoxins/PI stained renal tubules in collagen gel hollow fiber. (A) renal tubules with cross section view of right and bottom images sliced at the white dash lines, scale bar = 50 μm ; (B) 3D reconstructed confocal images, scale bar = 50 μm ; (C) zoom-in view showing cell–cell connection, scale bar = 20 μm .

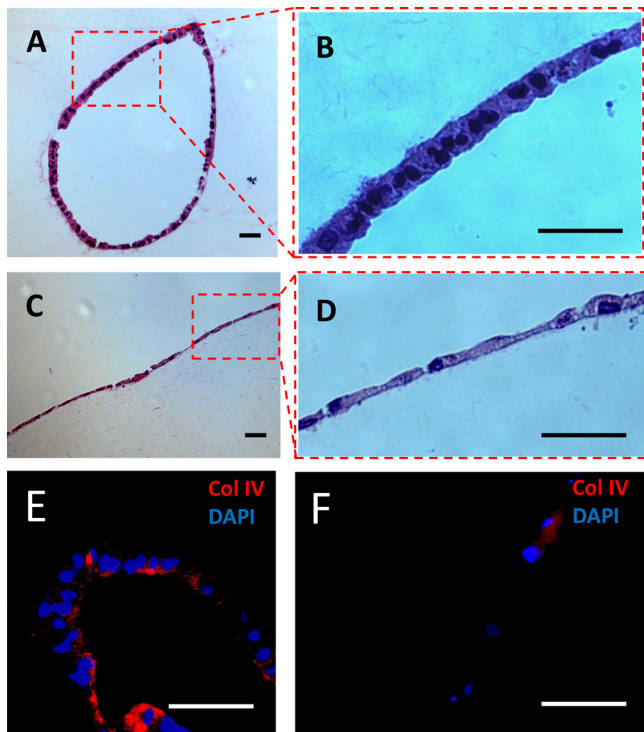


Figure 6. Hematoxylin–eosin staining of HK-2 cells in collagen gel hollow fiber (A and B) and on flat collagen gel (C and D) after 10 days of culture. Immunofluorescence staining of collagen IV (red) and DAPI (blue) on HK-2 cells in collagen gel hollow fiber (E) and on flat collagen gel (F). Scale bar = 50 μm .

spread more on flat collagen gel. The immunofluorescence staining similarly showed the denser nuclei and higher collagen IV expression in the renal tubule than that of the cells on the flat collagen gel (Figure E and F).

Functional Expression of Bioengineered Renal Tubules in Col HF. Bioengineered renal tubules with diameters of 200 μm were chosen for evaluation of cell function because of their higher cell amount and better diameter uniformity than

those with smaller diameters, which could provide higher accuracy in function detection. As shown in Figure 7A, the HK-2 cells in Col HF proliferated rapidly from Days 1 to 8 and then kept the cell density within Days 8 to 14, while the cells maintained high cell viability during the whole culture period (Figure 7A).

The functional expression of renal tubules was then detected and compared with the commonly used Transwell and HF membrane cultures. In Figure 7B, the HK-2 cells in Col HF culture expressed over 2-fold higher activity of brush border enzymes (ALP and GGT) than that of the Transwell culture and also 1-fold higher than that of the HF membrane culture. Consistently, the Col HF culture showed much higher MRP2 and GLUT activities than those of the two other cultures, as indicated by the 5-CFDA efflux and glucose uptake in HBSS, respectively (blue columns in Figure 7, parts C and D). Moreover, the Col HF culture was also more sensitive to the inhibitors of MRP2 efflux (probenecid, in Figure 7C) or glucose uptake (Na^+ -free and phlorizin, in Figure 7D).

The highly expressed renal functions in Col HF culture were confirmed by the RT-PCR assay (Figure 8). As shown in Figure 8A, each of the corresponding genes (*GLUT1/ALP/MRP2/GGT*) displayed higher expressions in Col HF culture than those in comparative cultures, consistent with the performances on their activities in Figure 7. The RT-PCR images were then digitized and analyzed by Image-Pro Plus software in Figure 8B. From this figure, the Col HF culture showed at least 1-fold higher gene expression level than each of the comparative culture.

DISCUSSION

The design of new scaffolds to form renal tubules is an interesting but challenging issue because of the great value in renal disease therapy. Collagen as an extracellular matrix is a desired material for forming such tubular scaffolds. Nevertheless, tubular-shaped collagen in the form of high density tubes²⁵ and dry HFs²⁶ could not provide a good microenvironment for cell culture as hydrogel, while the normal collagen hydrogel formed via the slow and weak thermo-gelling could not sustain a stable and strong HF shape in continuous fabrication (data not shown). The exposure of collagen hydrogel to chemical EDC cross-linking can stabilize the HF configuration by quickly forming amide covalent bonds between collagen molecules. As found in this paper, Col HFs after chemical cross-linking sustained an acceptable tensile strength (Young's modulus >0.2 MPa), consistent with collagen gel bulk by EDC cross-linking.^{15a} Further co-crosslinking Col HF with dendritic molecular^{15a} or poly(MPC-co-methacrylic acid)²⁷ will be expected to greatly improve the tensile strength to 1–5 MPa. Such mechanical properties were close to those of PDMS tubes²⁸ and sufficient for weaving into bunches like polymer HF membranes. In full consideration of biocompatibility, collagen-based HF could possibly replace synthetic HF membranes for future application in the tissue engineering.

Chemical cross-linkers were rarely used for fabricating cell-laden protein hydrogels because of their high cytotoxicity. To obtain good mechanical properties, the hydrogels need sufficient cross-linking by highly concentrated cross-linkers (>10 mM).^{15a,29} However, EDC and genipin performed the severe cytotoxicity with EC_{50} (the concentration that elicits 50% cell death) as low as about 0.5 mM (Figure 3A and Figure 3 in ref 30), while glutaraldehyde was even more toxic. Due to the large gap between the requirements of low toxicity and high

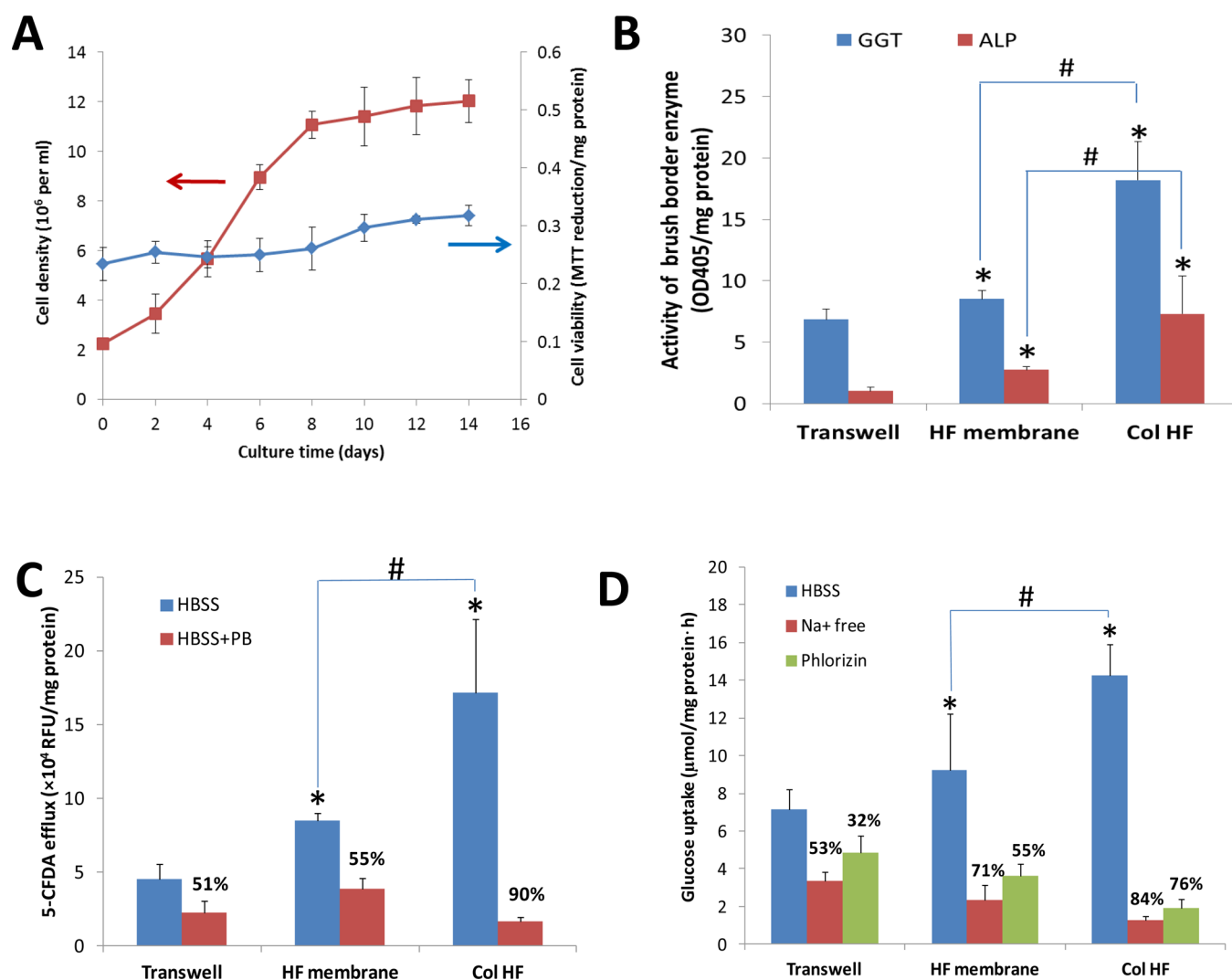


Figure 7. (A) Time-dependent alteration on cell density and viability during cell culture in Col HF. Functional assay of HK-2 cells in different cultures after 10 days of culture: (B) brush border enzymes (ALP&GGT) activity; (C) MRP2 activity represented by 5-CFDA efflux; (D) glucose uptake; * and # represent significant higher ($p < 0.05$) compared to the culture in Transwell and hollow fiber membrane, respectively. The percent data refer to the inhibited activity by corresponding inhibitors. Col HF = collagen gel hollow fiber; MTT = methyl thiazolyltetrazolium; ALP = alkaline phosphatase; GGT = γ -glutamyltransferase; PB = probenecid; and MRP2 = multidrug resistance protein 2.

mechanical properties, the chemically cross-linked cell-laden hydrogels became difficult and almost impossible. However, we delicately fabricated the cell-laden collagen gel by protecting the cells with the sacrificed Ca-alginate gel. The fast formed Ca-alginate gel may delay the EDC diffusion and thus greatly reduce the cell exposure to EDC. Also, the presence of the Ca-alginate core fiber helped to keep its configuration and enhance the mechanical property of Col HF (Figures 2 and 3). As Ca-alginate can be conveniently fabricated into various shapes (e.g., microsphere³¹ or fiber^{14b}) as well as liquefied by Ca^{2+} chelation, the strategy provided a universal concept in preparing differently shaped cell-laden lumens inside chemically cross-linked hydrogels.

The formation of in vivo-like tubules was closely related to the specific chemical and spatial microenvironments of Col HF. In view of chemical microenvironments, collagen is the most biocompatible material for cell culture. Although arginine-glycine-aspartic acid (RGD) as an integrin recognizing peptide has been well identified from collagen and further explored to greatly improve the cell adhesion/differentiation,³² collagen

itself still performs much better than RGD for stimulating the cell differentiated functions due to the contributions of other peptides.³³ But collagen as a chemical microenvironment, although necessary, was not sufficient for renal tubule formation. As a result, the renal cell culture on either the inner Col HF surface or the flat collagen gel surface, although with the same chemical components, formed completely different cell morphologies (Figure 6). Besides, the 3D tubules in Col HF had a cell thickness of 10 μm , which approached the thickness of renal tubular cells in human kidney (about 10 μm),³⁴ while the 2D monolayer on the flat collagen gel showed a cell thickness of only 3–5 μm (Figure 6). Similarly, the renal tubular cells, when simply entrapped inside a homogeneous collagen gel, could not form tubules,^{13a,b,35} while the MDCK cells, when seeded on a grooved collagen-matrigel hydrogel, could self-assemble into short tubular structure.³⁶ In this regard, the tubular shaped Col HF seemed to create a microenvironment that was more similar to that found under in vivo conditions, and thus provided a good template for leading to the renal tubule formation.

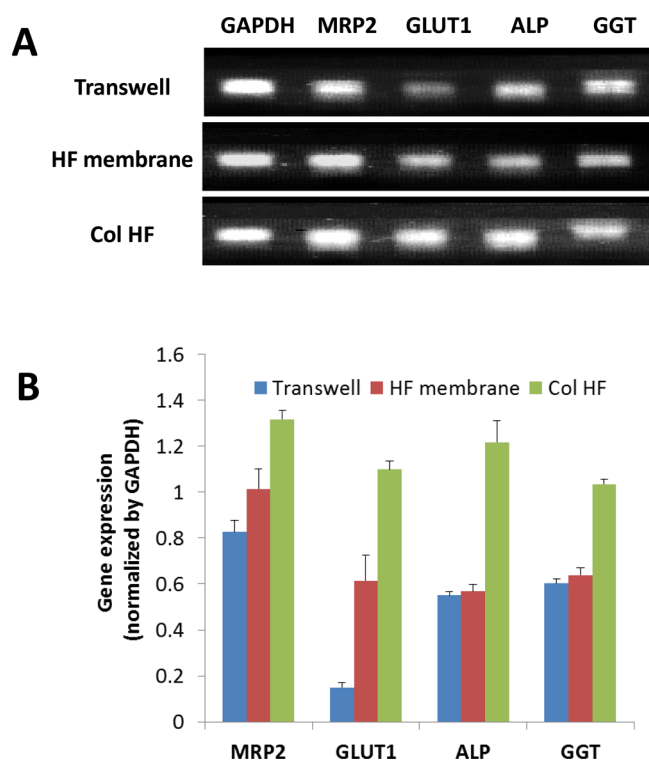


Figure 8. RT-PCR assay of gene expression of *ALP*, *GGT*, *GLUT*, and *MRP2*, while *GAPDH* was used as the house-keeping gene. (A) Gel electrophoresis image of RT-PCR assay; (B) data were digitized from images by Image Pro Plus 6.0. *ALP* = alkaline phosphatase; *GGT* = γ -glutamyltransferase; *MRP2* = multidrug resistance protein 2; *GLUT1* = glucose transporter 1; and *GAPDH* = glyceraldehyde-3-phosphate dehydrogenase.

Hence, we assumed that the *in vivo*-like tubular morphology of the bioengineered renal tubules can stimulate their performances on renal function. HK-2 cells in Col HF culture not only well differentiated according to the high performance on *ALP* & *GGT* activity,¹⁶ but also showed good reabsorptive ability of renal tubules, reflected by the high *MRP2* and *GLUT* activity.¹⁷ Our previous results have found that the renal cell layers expressed higher renal functions on polysulfone HF than those on flat polysulfone membrane, while smaller diameters of HF from 800 to 400 μm further up-regulated differential functions of the cell layers.¹⁹ In this study, the increased substrate curvature (Transwell < HF membrane < Col HF) may also show positive effects on improving renal function (Figures 7 and 8). Because the renal tubules in the kidney are of small diameter at about 50 μm ,³⁷ we expect that the functions of renal tubules in Col HF will be negatively related with their diameters at a sequence of 200 μm < 100 μm < 50 μm .

The bioengineered renal tubules in Col HF comprise only cells and collagen, exclusive of any synthetic materials. This offers the high possibility of a bioartificial kidney as an implantable device and suggests a novel design of bioartificial organs. Such a new device with high renal function would allow prolonged and continuous treatment in clinic, which is expected to improve the therapy efficacy and patients' treatment experience.⁵ Another valuable application of bioengineered renal tubules could be in the pharmaceutical field. Similar to the renal cell organoids, which showed a more physiologically relevant response to nephrotoxicity than that of the renal cells at normal 2D culture,³⁸ the bioengineered renal

tubules with uniquely high function (Figures 7 and 8) could be a better platform for high-throughput screening of drug nephrotoxicity.

CONCLUSIONS

This study presented a novel method to fabricate renal tubules by culturing renal cells in Col HF. With the delicate design of Ca-alginate as the sacrificial cores, renal tubular cells were loaded in the lumen of Col HF with acceptable mechanical strength properties. Within 10 days of culture, the HK-2 in Col HF self-assembled into intact renal tubular structures with diameters of 50–200 μm . Such renal tubules expressed at least 1-fold higher renal function than the renal cells on Transwell or polymer HF membranes. The bioengineered renal tubules possess great potential in the clinical therapy of end-stage kidney disease and on the establishment of a platform for high-throughput screening of drug nephrotoxicity.

AUTHOR INFORMATION

Corresponding Author

*Tel: 86-571-87953193; fax: 86-571-87951227; e-mail: mengq@zju.edu.cn (Q.M.).

Notes

The authors declare no competing financial interest.

ACKNOWLEDGMENTS

We gratefully acknowledge the financial support of this study by NSFC (National Natural Science Foundation of China, Nos. 21476197 and 21276227). We thank Prof. Libera at Stevens Institute of Technology (New Jersey, U.S.A.) for providing the confocal microscope and Dr. Li Jiang in Chongqing University of Medical Sciences (Chongqing, China) for help with the microfluidic fabrication. We also thank Zhang Yufan at University of California, Berkeley for his help on language editing.

REFERENCES

- (1) Kermanizadeh, A.; Gaiser, B. K.; Ward, M. B.; Stone, V. Primary human hepatocytes versus hepatic cell line: assessing their suitability for *in vitro* nanotoxicology. *Nanotoxicology* **2013**, *7* (7), 1255–71.
- (2) Humes, H. D.; Buffington, D.; Westover, A. J.; Roy, S.; Fissell, W. H. The bioartificial kidney: current status and future promise. *Pediatr. Nephrol.* **2014**, *29*, 343.
- (3) Go, A. S.; Chertow, G. M.; Fan, D.; McCulloch, C. E.; Hsu, C. Y. Chronic kidney disease and the risks of death, cardiovascular events, and hospitalization. *N. Engl. J. Med.* **2004**, *351* (13), 1296–305.
- (4) Humes, H. D.; Buffington, D. A.; MacKay, S. M.; Funke, A. J.; Weitzel, W. F. Replacement of renal function in uremic animals with a tissue-engineered kidney. *Nat. Biotechnol.* **1999**, *17* (5), 451–5.
- (5) (a) Tasnim, F.; Deng, R.; Hu, M.; Liour, S.; Li, Y.; Ni, M.; Ying, J. Y.; Zink, D. Achievements and challenges in bioartificial kidney development. *Fibrog. Tissue Repair* **2010**, *3*, 14. (b) Tumlin, J.; Wali, R.; Williams, W.; Murray, P.; Tolwani, A. J.; Vinnikova, A. K.; Szerlip, H. M.; Ye, J.; Paganini, E. P.; Dworkin, L.; Finkel, K. W.; Kraus, M. A.; Humes, H. D. Efficacy and safety of renal tubule cell therapy for acute renal failure. *J. Am. Soc. Nephrol.* **2008**, *19* (5), 1034–40.
- (6) (a) Zhang, H.; Tasnim, F.; Ying, J. Y.; Zink, D. The impact of extracellular matrix coatings on the performance of human renal cells applied in bioartificial kidneys. *Biomaterials* **2009**, *30* (15), 2899–911. (b) Oo, Z. Y.; Deng, R.; Hu, M.; Ni, M.; Kandasamy, K.; bin Ibrahim, M. S.; Ying, J. Y.; Zink, D. The performance of primary human renal cells in hollow fiber bioreactors for bioartificial kidneys. *Biomaterials* **2011**, *32* (34), 8806–15.
- (7) Ni, M.; Teo, J. C.; Ibrahim, M. S.; Zhang, K.; Tasnim, F.; Chow, P. Y.; Zink, D.; Ying, J. Y. Characterization of membrane materials and

membrane coatings for bioreactor units of bioartificial kidneys. *Biomaterials* **2011**, *32* (6), 1465–76.

(8) Ueda, H.; Watanabe, J.; Konno, T.; Takai, M.; Saito, A.; Ishihara, K. Asymmetrically functional surface properties on biocompatible phospholipid polymer membrane for bioartificial kidney. *J. Biomed. Mater. Res., Part A* **2006**, *77* (1), 19–27.

(9) Miner, J. H. Renal basement membrane components. *Kidney Int.* **1999**, *56* (6), 2016–24.

(10) Alexander, L. D.; Alagarsamy, S.; Douglas, J. G. Cyclic stretch-induced cPLA2 mediates ERK 1/2 signaling in rabbit proximal tubule cells. *Kidney Int.* **2004**, *65* (2), 551–63.

(11) Nony, P. A.; Nowak, G.; Schnellmann, R. G. Collagen IV promotes repair of renal cell physiological functions after toxicant injury. *American journal of physiology. Renal physiology* **2001**, *281* (3), F443–53.

(12) Walters, B. D.; Stegemann, J. P. Strategies for directing the structure and function of three-dimensional collagen biomaterials across length scales. *Acta Biomater.* **2013**, *10*, 1488.

(13) (a) Montesano, R.; Schaller, G.; Orci, L. Induction of epithelial tubular morphogenesis in vitro by fibroblast-derived soluble factors. *Cell* **1991**, *66* (4), 697–711. (b) Bao, Q.; Hughes, R. C. Galectin-3 expression and effects on cyst enlargement and tubulogenesis in kidney epithelial MDCK cells cultured in three-dimensional matrices in vitro. *J. Cell Sci.* **1995**, *108* (8), 2791–800. (c) Jiang, S. T.; Chiu, S. J.; Chen, H. C.; Chuang, W. J.; Tang, M. J. Role of alpha(3)beta(1) integrin in tubulogenesis of Madin-Darby canine kidney cells. *Kidney Int.* **2001**, *59* (5), 1770–8. (d) Jiang, S. T.; Chuang, W. J.; Tang, M. J. Role of fibronectin deposition in branching morphogenesis of Madin-Darby canine kidney cells. *Kidney Int.* **2000**, *57* (5), 1860–7.

(14) (a) Onoe, H.; Okitsu, T.; Itou, A.; Kato-Negishi, M.; Gojo, R.; Kiriya, D.; Sato, K.; Miura, S.; Iwanaga, S.; Kuribayashi-Shigetomi, K.; Matsunaga, Y. T.; Shimoyama, Y.; Takeuchi, S. Metre-long cell-laden microfibrils exhibit tissue morphologies and functions. *Nat. Mater.* **2013**, *12* (6), 584–90. (b) Hu, M.; Deng, R.; Schumacher, K. M.; Kurisawa, M.; Ye, H.; Purnamawati, K.; Ying, J. Y. Hydrodynamic spinning of hydrogel fibers. *Biomaterials* **2010**, *31* (5), 863–9.

(15) (a) Duan, X.; Sheardown, H. Dendrimer crosslinked collagen as a corneal tissue engineering scaffold: Mechanical properties and corneal epithelial cell interactions. *Biomaterials* **2006**, *27* (26), 4608–4617. (b) Sundararaghavan, H. G.; Monteiro, G. A.; Lapin, N. A.; Chabal, Y. J.; Miksan, J. R.; Shreiber, D. I. Genipin-induced changes in collagen gels: correlation of mechanical properties to fluorescence. *J. Biomed. Mater. Res., Part A* **2008**, *87* (2), 308–20.

(16) Westhuyzen, J.; Endre, Z. H.; Reece, G.; Reith, D. M.; Saltissi, D.; Morgan, T. J. Measurement of tubular enzymuria facilitates early detection of acute renal impairment in the intensive care unit. *Nephrology, dialysis, transplantation: official publication of the European Dialysis and Transplant Association - European Renal Association* **2003**, *18* (3), 543–51.

(17) Pfaller, W.; Gstraunthaler, G. Nephrotoxicity testing in vitro—what we know and what we need to know. *Environ. Health Perspect.* **1998**, *106* (2), 559–69.

(18) Duffy, D. C.; McDonald, J. C.; Schueller, O. J.; Whitesides, G. M. Rapid Prototyping of Microfluidic Systems in Poly(dimethylsiloxane). *Anal. Chem.* **1998**, *70* (23), 4974–84.

(19) Shen, C.; Meng, Q.; Zhang, G. Increased curvature of hollow fiber membranes could up-regulate differential functions of renal tubular cell layers. *Biotechnol. Bioeng.* **2013**, *110* (8), 2173–83.

(20) Bessey, O. A.; Lowry, O. H.; Brock, M. J. A method for the rapid determination of alkaline phosphates with five cubic millimeters of serum. *J. Biol. Chem.* **1946**, *164*, 321–9.

(21) Szasz, G. A Kinetic Photometric Method for Serum Gamma-Glutamyl Transpeptidase. *Clin. Chem.* **1969**, *15* (2), 124.

(22) Payen, L.; Delugin, L.; Courtois, A.; Trinquart, Y.; Guillouzo, A.; Fardel, O. The sulphonylurea glibenclamide inhibits multidrug resistance protein (MRP1) activity in human lung cancer cells. *Br. J. Pharmacol.* **2001**, *132* (3), 778–84.

(23) Humes, H. D.; Fissell, W. H.; Weitzel, W. F.; Buffington, D. A.; Westover, A. J.; MacKay, S. M.; Gutierrez, J. M. Metabolic replacement

of kidney function in uremic animals with a bioartificial kidney containing human cells. *Am. J. Kidney Dis.* **2002**, *39* (5), 1078–87.

(24) Wilkening, S.; Bader, A. Influence of culture time on the expression of drug-metabolizing enzymes in primary human hepatocytes and hepatoma cell line HepG2. *J. Biochem. Mol. Toxicol.* **2003**, *17* (4), 207–13.

(25) Micol, L. A.; Ananta, M.; Engelhardt, E. M.; Mudera, V. C.; Brown, R. A.; Hubbell, J. A.; Frey, P. High-density collagen gel tubes as a matrix for primary human bladder smooth muscle cells. *Biomaterials* **2011**, *32* (6), 1543–8.

(26) Viswanadham, R. K.; Kramer, E. J. Structure of Reconstituted Collagen Hollow Fiber Membranes. *J. Mater. Sci.* **1975**, *10* (9), 1472–1480.

(27) Nam, K.; Kimura, T.; Funamoto, S.; Kishida, A. Preparation of a collagen/polymer hybrid gel designed for tissue membranes. Part I: controlling the polymer-collagen cross-linking process using an ethanol/water co-solvent. *Acta Biomater.* **2010**, *6* (2), 403–8.

(28) *Polymer Data Handbook*; Oxford University Press, Inc.: Oxford, UK, 1999.

(29) Powell, H. M.; Boyce, S. T. EDC cross-linking improves skin substitute strength and stability. *Biomaterials* **2006**, *27* (34), S821–7.

(30) Fessel, G.; Cadby, J.; Wunderli, S.; van Weeren, R.; Snedeker, J. G. Dose- and time-dependent effects of genipin crosslinking on cell viability and tissue mechanics - toward clinical application for tendon repair. *Acta Biomater.* **2014**, *10* (5), 1897–906.

(31) Capone, S. H.; Dufresne, M.; Rechel, M.; Fleury, M. J.; Salsac, A. V.; Paullier, P.; Daujat-Chavanieu, M.; Legallais, C. Impact of alginate composition: from bead mechanical properties to encapsulated HepG2/C3A cell activities for in vivo implantation. *PLoS One* **2013**, *8* (4), e62032.

(32) (a) De Bartolo, L.; Morelli, S.; Lopez, L. C.; Giorno, L.; Campana, C.; Salerno, S.; Rende, M.; Favia, P.; Detomaso, L.; Gristina, R.; d'Agostino, R.; Drioli, E. Biotransformation and liver-specific functions of human hepatocytes in culture on RGD-immobilized plasma-processed membranes. *Biomaterials* **2005**, *26* (21), 4432–41. (b) Hersel, U.; Dahmen, C.; Kessler, H. RGD modified polymers: biomaterials for stimulated cell adhesion and beyond. *Biomaterials* **2003**, *24* (24), 4385–415.

(33) Singh, R. K.; Seliktar, D.; Putnam, A. J. Capillary morphogenesis in PEG-collagen hydrogels. *Biomaterials* **2013**, *34* (37), 9331–40.

(34) Schaub, T. P.; Kartenbeck, J.; Konig, J.; Spring, H.; Dorsam, J.; Staehler, G.; Storkel, S.; Thon, W. F.; Keppler, D. Expression of the MRP2 gene-encoded conjugate export pump in human kidney proximal tubules and in renal cell carcinoma. *Journal of the American Society of Nephrology: JASN* **1999**, *10* (6), 1159–69.

(35) Jiang, S. T.; Chiang, H. C.; Cheng, M. H.; Yang, T. P.; Chuang, W. J.; Tang, M. J. Role of fibronectin deposition in cystogenesis of Madin-Darby canine kidney cells. *Kidney Int.* **1999**, *56* (1), 92–103.

(36) Schumacher, K. M.; Phua, S. C.; Schumacher, A.; Ying, J. Y. Controlled formation of biological tubule systems in extracellular matrix gels in vitro. *Kidney Int.* **2008**, *73* (10), 1187–92.

(37) (a) Jameson, J. L.; Loscalzo, J. *Harrison's Nephrology and Acid-Base Disorders*; McGraw-Hill Companies, Inc.: New York, 2010. (b) Niimi, K.; Yasui, T.; Hirose, M.; Hamamoto, S.; Itoh, Y.; Okada, A.; Kubota, Y.; Kojima, Y.; Tozawa, K.; Sasaki, S.; Hayashi, Y.; Kohri, K. Mitochondrial permeability transition pore opening induces the initial process of renal calcium crystallization. *Free Radical Biol. Med.* **2012**, *52* (7), 1207–1217.

(38) Astashkina, A. I.; Mann, B. K.; Prestwich, G. D.; Grainger, D. W. A 3-D organoid kidney culture model engineered for high-throughput nephrotoxicity assays. *Biomaterials* **2012**, *33* (18), 4700–11.